

Non-Linear and Multi-Domain Modelling of an Opposed-Piston Free Piston Engine during Motoring

Patrick Brosnan¹, Guohong Tian^{1*} Umberto Montanaro¹, Sam Cockerill²

¹ University of Surrey, Guildford, Surrey, GU2 7XH, UK (*Corresponding Author: g.tian@surrey.ac.uk).

² Libertine Ltd, Tinsley, Sheffield, S9 1DA, UK.

ABSTRACT

When coupling the Free Piston Engine (FPE) to the Permanent Magnet Linear Synchronous Machine (PMLSM) to produce electrical energy, its intrinsic multi-directional and non-linear dynamics have been typically described in a simplified mono-directional and linear fashion when considering a system-level modelling approach.

This paper presents a detailed, multi-directional, multi-domain model of the FPE and PMLSM. The model was implemented in an opposed-piston free-piston engine configuration and validated against experimental data captured from a prototype with identical parameters. The simulation results indicate a strong correlation to the experimental data, which captured the dominant dynamics of the FPE and proved the satisfactory accuracy and performance of the model.

This study considers the characteristic multi-directional nature and non-linearity of the machine dynamics and its interactions with multi-physical domains such as electrical, mechanical, and pneumatic.

Keywords: free-piston engine (FPE), permanent magnet linear synchronous machine (PMLSM), non-linear modelling, multi-domain modelling, in-cylinder modelling

NONMENCLATURE

Abbreviations

FPE	Free-Piston Engine
PMLSM	Permanent Magnet Linear Synchronous Machine
CPE	Conventional Piston Engine
RESS	Rechargeable Energy Storage System

Symbols

A	Area [m^2]
C_d	Discharge Coefficient
Ψ	Flux Linkage [Wb]
F	Force [N]

γ	Specific Heat Ratio
H	Enthalpy [J]
i	Current [A]
K_f	Force Constant [N/A]
L	Inductance [H]
m	Mass of Gas Mixture [kg]
\dot{m}	Mass Flow Rate of Mixture [kg/s]
M	Mass of Solid [kg]
P	Absolute Pressure [bar]
Q	Thermal Heat Energy [J]
R_s	Resistance [Ω]
T	Temperature [K]
V	Volume [m^3]
v	Voltage [v]
x_m	Translator Position [m]
\dot{x}_m	Translator Velocity [m/s]
\ddot{x}_m	Translator Acceleration [m/s^2]

1. INTRODUCTION

Modern times have been a motivational driver and enabler of low carbon emissions technology development.

Global carbon emissions reduction can be considered a worldwide challenge, with industry and academia actively engaged in developing a viable solution. In the modern era, with the rapid technological advances in low carbon solutions, renewed interest and development in future thermal propulsion technologies such as the Free Piston Engine (FPE) have increased [1–3].

Technological institutes, as well as industry led by private companies, are investigating the applications and usefulness of the FPE as a practical solution to reduce in-cylinder combustion emissions. The FPE is a unique thermal hybrid propulsion machine with a higher thermal efficiency than its counterpart, the Conventional Reciprocating Piston Engine (CPE). Moreover, the system dynamics intrinsically influence the piston motion,

advantages of which can lead to the optimisation of several operational modes [4,5].

1.1 Existing Research

The research presented in the FPE modelling literature focuses on a mono-directional and linear description of the machine dynamics. The following key studies have conducted a system-level and control-orientated approach describing the machine dynamics during motoring and power generation [6–12].

The majority of the FPE PMLSM research recognised that a linear mathematical description of the FPE is computationally cheap and can be used in a system-level approach. However, they may fail to describe the characteristic multi-directional and non-linear load interactions fully. Furthermore, previous FPE system-level studies did not account for the non-linearity of the PMLSM, preferring to describe the dynamics in a simplified linear fashion. The key novelty in this study is the inherent non-linearities of the FPE, and PMLSM itself will be considered.

The paper aims to present the initial findings of an opposed-piston FPE modelling study, furthermore, one that considers a non-linear and system-level modelling approach.

2. OPPOSED-PISTON FPE MODELLING

The FPE, including the PMLSM, can be described as operating in two distinct modes, motoring mode (motor) and generating mode (generator), whereby the electromagnetic force produces an oscillatory translational motion (linear in this sense) [13]. The energy flow of the proposed model is illustrated below in Fig. 1 [14].

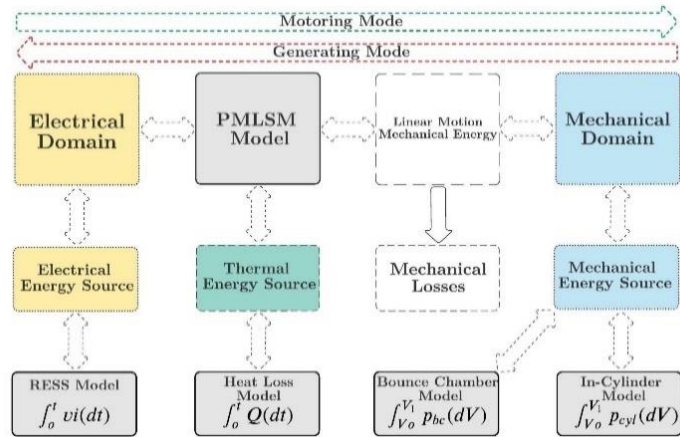


Fig. 1 FPE Energy Flow Schematic

where the electrical domain variables v and i (orange blocks) are voltage and current, the mechanical domain variables V and p (blue blocks) are cylinder volume and pressure, respectively. The thermal domain variable Q is the stator thermal energy flow. In addition, the models describing the PMLSM, Rechargeable Energy Storage System (RESS), heat loss, and bounce chambers (grey blocks) were created in SimScape and the in-cylinder model in Simulink.

The opposed-piston FPE architecture is considered and presented in this study, as illustrated below in Fig. 2.

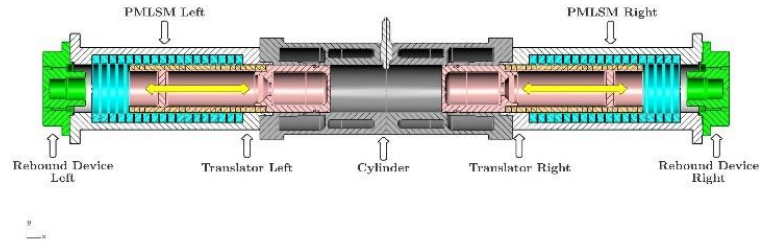


Fig. 2 Opposed-Piston FPE Schematic

The main components highlighted above in Fig. 2 include the rebound device, in this case, a pneumatic Bounce Chamber (BC), the PMLSM, the translator (piston and rotor assembly), and the cylinder assembly.

The equivalent three-phase electrical circuit, the translational mechanical circuit, thermal circuit, and thermodynamic load circuit of the proposed opposed-piston FPE model with its characteristic multi-directional architecture is illustrated below in Fig. 3. A detailed description of the Simscape variables is given in [15,16].

2.1 Non-Linear PMLSM Mathematical Description

This study applies the established Clarke Park $dq0$ reference frame transform to the three-phase stator dynamics and yields the following [17,18]:

$$L_d \frac{di_d}{dt} = v_d - R_s i_d + N_p i_q L_q \dot{x}_m \quad (1)$$

$$L_q \frac{di_q}{dt} = v_q - R_s i_q - N_p \dot{x}_m (i_d L_d + \Psi_{pm}) \quad (2)$$

$$L_0 \frac{di_0}{dt} = v_0 - R_s i_0 \quad (3)$$

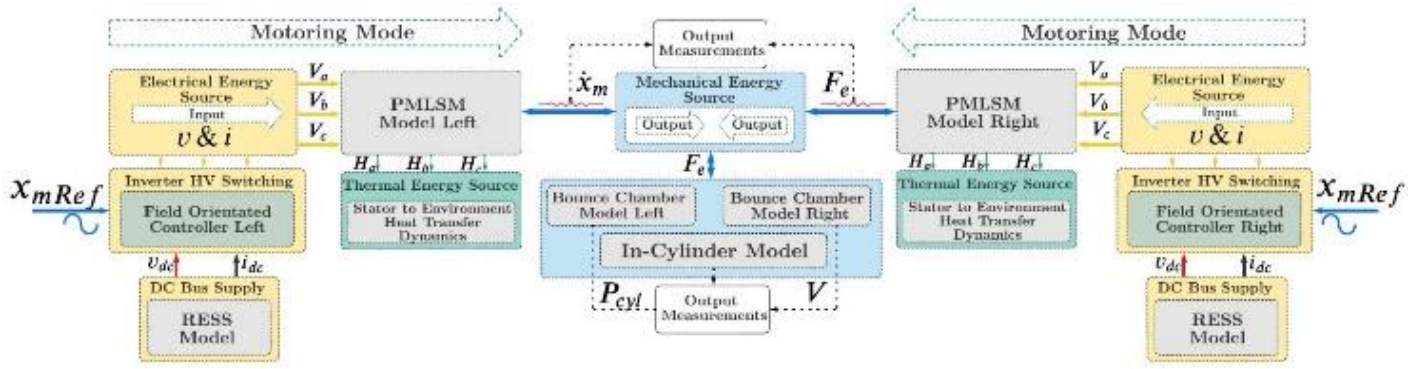


Fig. 3 Opposed-Piston FPE Motoring Model Schematic

where first, v_d, v_q and v_0 are the transformed stator d, q and 0 axis voltages, second, R_s is the idealised resistance in the stator, third, i_d, i_q and i_0 are the stator d, q and 0 axis currents, fourth, L_d, L_q and L_0 are the stator inductances, fifth, Ψ the flux linkage and finally, N_p is the pole pitch factor.

In addition, applying the Clarke Park $dq0$ transform to the electric force F_e description yields the following:

$$F_e = \frac{3}{2} N_p [i_q (i_d L_d + \Psi_{pm}) - i_d i_q L_q] \quad (4)$$

2.1.1 Mechanical Dynamics

The mechanical forces experienced by each FPE translator are described by Newton's 2nd law of motion, relating the electric machine rotor force F_e and rotor acceleration (translator) \dot{x}_m as:

$$M \dot{x}_m = F_e - F_{cyl} - F_{fr} + F_{bc} \quad (5)$$

where $M, \dot{x}_m, F_{cyl}, F_{fr}$, and F_{bc} are the translator mass (piston and rotor assembly), translator acceleration, the in-cylinder force as acting upon the translator, the total damping forces as acting upon the translator, and the bounce chamber force, respectively.

2.2 In-Cylinder Mathematical Modelling

This study presents a zero-dimensional and single-zone model that describes the in-cylinder gas temperature, pressure, mass, and energy evolution over a two-stroke cycle and assumes the composition to be uniform and homogeneous throughout.

Represented mathematically and assuming the in-cylinder gases obey the ideal gas law, with the constant

volume specific heat constant C_v and the gas constant R_g as continuous throughout the process, it can be shown [13,19]:

$$\frac{dU}{dt} = \frac{dQ}{dt} - P \frac{dV}{dt} + \sum \dot{H}_i - \sum \dot{H}_e \quad (6)$$

where $\frac{dU}{dt}$ is the time derivative of internal energy, $\frac{dV}{dt}$ is the time derivative of volumetric work, $\frac{dQ}{dt}$ is the time derivative of heat addition and loss of the system, H_i is the inlet charge enthalpy, and H_e is the exhaust gas enthalpy.

Heat addition and loss in the closed in-cylinder process consist of heat energy added to the system through combustion and heat loss to the system through heat transfer. In this case, the total heat energy loss is shown as:

$$\frac{dQ}{dt} = - \frac{dQ_{HT}}{dt} \quad (7)$$

where Q_{HT} is the heat loss energy.

2.2.1 Compression and Expansion Process

Applying the first law of thermodynamics can show the time evolution of the in-cylinder pressure P as [13]:

$$\begin{aligned} \frac{dP}{dt} = & - \left[\frac{\gamma - 1}{V} \right] - \left[\frac{dQ_{HT}}{dt} \right] - \gamma \left[\frac{P}{V} \right] \left[\frac{dV}{dt} \right] \\ & - \left[\frac{p\gamma}{m_{air}} \right] \left[\frac{dm_{air}}{dt} \right] + \left[\frac{\gamma - 1}{V} \right] \sum_i m_i h_i \end{aligned} \quad (8)$$

where $\gamma = \frac{C_p}{C_v}$ is the specific heat ratio and C_p is the constant pressure specific heat constant.

The net air in-cylinder mass flow rate can be shown as $\dot{m}_{air} = \dot{m}_{in} - \dot{m}_{ex} - \dot{m}_l$. Where \dot{m}_{in} , \dot{m}_{ex} , \dot{m}_l are the mass flow rate through the intake ports, the mass flow rate through the exhaust ports, and the mass flow rate past the piston ring pack.

2.3 Gas Exchange Process

The intake mass flow rate \dot{m}_{in} and exhaust mass flow rate \dot{m}_{ex} through the scavenging ports (uni-flow port configuration) are determined by the discharge area, which in the case of the intake mass flow rate is shown as A_{in} , the intake discharge coefficient C_d and the upstream and downstream cylinder pressure p_u and p_d , respectively [19,20].

2.4 Heat Loss

The idealised heat loss through the cylinder walls, assuming uniform and quasi-steady behaviour described as [19,21]:

$$\dot{Q}_{HT} = h_t A_{cyl}(T - T_{wall}) \quad (9)$$

where h_t is the heat transfer coefficient described by the Woschni correlation, A_{cyl} is the cylinder surface area and T_{wall} is the chamber surface temperature. The Hohenberg extended Woschni correlation is shown as [22]:

$$h = C_1 V_{cyl}^{-0.06} \left[\frac{p_u}{10^5} \right]^{0.8} T^{-0.4} (\dot{x}_m + C_2)^{0.8} \quad (10)$$

where, C_1 and C_2 are constants, V_{cyl} is the instantaneous cylinder volume, p_u and T are upstream pressure and temperature, respectively, and \dot{x}_m the average piston velocity.

2.5 Friction

The net friction F_{fr} is described as that from the contact of the piston ring pack to the cylinder $F_{fr_{cyl}}$, the contact friction seen by the PMLSM rotor $F_{fr_{re}}$ and the bounce chamber ring pack $F_{fr_{bc}}$ and is shown as:

$$F_{fr} = F_{fr_{cyl}} + F_{fr_{re}} + F_{fr_{bc}} \quad (11)$$

Describing the PMLSM friction $F_{fr_{re}}$ due to contact between the rotor and stator, the friction of the bounce chamber $F_{fr_{bc}}$ due to contact between the piston sealing ring and bore are both assumed to be constant due to the relatively low piston velocity seen by the FPE,

shown as $F_{fr_{re}} = -C_e \text{sign}(\dot{x}_m)$ and $F_{fr_{bc}} = -C_{bc} \text{sign}(\dot{x}_m)$, respectively.

where C_e and C_{bc} are friction constants for the electric machine and bounce chamber, respectively, and $\text{sign}(\dot{x}_m)$ is the direction of the translator velocity.

The piston ring friction force is due to the tension in the compression ring and the oil control ring against the cylinder bore. In addition, the in-cylinder gas pressure acts upon the piston, creating pressure on the rear and top faces of the rings, producing a radial force [23].

3. MOTORING CONTROL

Implementation of a model-based motoring control scheme was conducted in Simscape. This study selected a control objective of piston position tracking for model validation, whereby a linear cascaded control architecture was designed, optimised, and employed.

4. MODEL VALIDATION

Concerning validation of the FPE model as described above in Section 2, experimental test data was captured from a rig-mounted prototype opposed-piston FPE, as presented below in Fig. 4 [24].

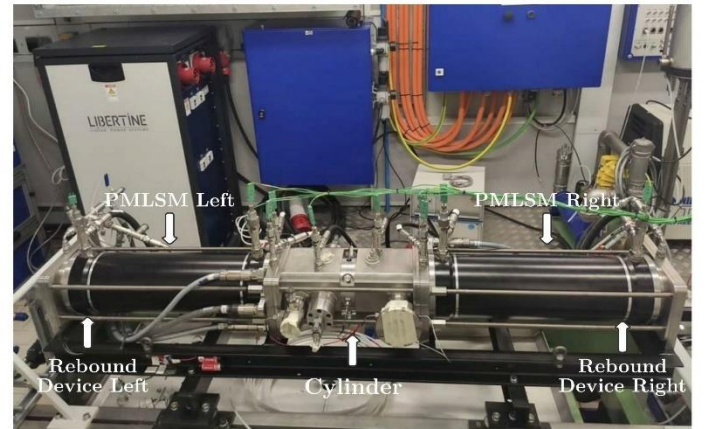


Fig. 4 Opposed-Piston FPE Experimental Test

The experimental hardware was fed with a Direct Current (DC) bus supply voltage of 600 v and operated at a target frequency of 18.5 Hz. Additionally, the FPE experimental parameters are presented below in Table 1.

Table 1. Opposed-Piston FPE Experimental Parameters

	Parameters	Symbol	Value
System	Operating Frequency	f	18.5 Hz
	PWM Frequency	f_{sw}	8.0 KHz
	DC Bus Voltage	v_{dc}	600 v
	FPE	Cylinder Bore	B
	Max Displacement	x_{max}	0.133 m
	Compression Ratio	CR	11.5:1
	Air Intake Pressure	p_{in}	1.2 bar
	BC Supply Pressure	p_{bc}	0.6 bar
PMLSM	Armature Resistance	R_s	1.5 Ω
	Armature Inductance	L_s	0.011 H
	Pole Pitch	τ	0.08 m
	Translator Mass	M	6.0 kg
	Viscous Damping	C_e	250 kg/s
	Max Stator Current	i_{max}	120 A

4.1 Results

Fig. 5 above presents the correlation between the proposed non-linear and multi-domain FPE model and FPE experimental data. The qualitative comparison indicates that the observed model results are similar to the experimental results. Most importantly, the proposed model described in Section 2 can capture the mechanical and thermodynamic performance of the FPE, which is essential for a model to be implemented in a system-level model and represent the machine's dominant non-linear dynamics.

5. CONCLUSION

This study set out to fill the gap in the current FPE literature concerning describing the dynamics of the FPE in a multi-directional, non-linear, and multi-domain fashion. Consequently, a non-linear and multi-domain equivalent opposed-piston FPE model was first presented, followed by a mathematical description of the dynamics. Finally, this study demonstrated the

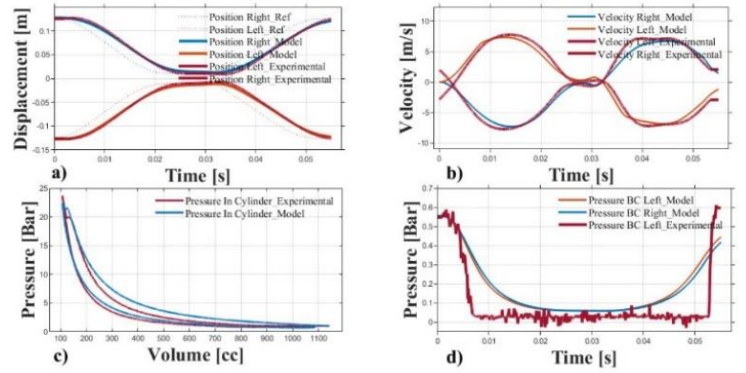


Fig. 5 Validation Results: a) Displacement x_m [m], b) Velocity \dot{x}_m [m/s], c) In-Cylinder Pressure p_{cyl} [bar], d) Bounce Chamber Pressure p_{bc} [bar]

proposed FPE model to assess its functionality and performance.

The qualitative validation presented the relationship between the experimental data and model data, demonstrating that the proposed model captured the experimental hardware's dominant dynamics and satisfied the key focus set out in this study. Furthermore, the model naturally considered the non-linearity of the machine dynamics and interactions with multi-physical domains. This demonstrated that the proposed model could be incorporated and implemented in a modelling approach that considers system-level design.

ACKNOWLEDGEMENT

This work is supported by the royal society project IEC/NSFC/181025 for Investigation of Free Piston Generators for Vehicle Applications and Libertine FPE Limited. In addition, the authors would like to thank MathWorks Martina Sciola and Sabin Carpiuc for their help and support during the PMLSM modelling phase of this project.

REFERENCE

- [1] A. L. London. Free-Piston and Turbine Compound Engine - Status of the Development. SAE Transcript 1954;62:426–36.
- [2] J. G. Coutant. Four-stage Free-piston Compressor. Soc Am Mil Eng 1960;52:302–4.
- [3] Philip L. Scott. Construction of Junkers Engine. SAE Int 1917;12, Part I:404–24.
- [4] Feng H, Guo Y, Song Y, Guo C, Zuo Z. Study of the Injection Control Strategies of a Compression Ignition Free Piston Engine Linear Generator in a One-Stroke Starting Process. Energies 2016;9:453. <https://doi.org/10.3390/en9060453>.

- [5] Huang L, Xu Z. An opposed-piston free-piston linear generator development for HEV. SAE Tech Paper2012.<https://doi.org/10.4271/2012-01-1021>.
- [6] Johansen TA, Egeland O, Johannessen EA, Kvamsdal R. Dynamics and control of a free-piston diesel engine. J Dyn Syst Meas Control TransASME2003;125:468–74. <https://doi.org/10.1115/1.1589035>.
- [7] Bergman M, Fredriksson J, Golovitchev VI. CFD-based optimization of a diesel-fueled free piston engine prototype for conventional and HCCI combustion. SAE Int J Engines 2009;1:1118–43. <https://doi.org/10.4271/2008-01-2423>.
- [8] Mikalsen R, Jones E, Roskilly AP. Predictive piston motion control in a free-piston internal combustion engine. Appl Energy 2010;87:1722–8. <https://doi.org/10.1016/j.apenergy.2009.11.005>.
- [9] Li K, Sadighi A, Sun Z. Active Motion Control of a HydraulicFreePistonEngine.2014;90:375. <https://doi.org/10.2307/3950417>.
- [10] Jia B, Mikalsen R, Smallbone A, Zuo Z, Feng H, Roskilly AP. Piston motion control of a free-piston engine generator: A new approach using cascade control.ApplEnergy2016;179:1166–75. <https://doi.org/10.1016/j.apenergy.2016.07.081>.
- [11] Jia B, Smallbone A, Feng H, Tian G, Zuo Z, Roskilly AP. A fast response free-piston engine generator numerical model for control applications. Appl Energy2016;162:321–9. <https://doi.org/10.1016/j.apenergy.2015.10.108>.
- [12] Gong X, Zaseck K, Kolmanovsky I, Chen H. Modeling and Predictive Control of Free Piston Engine Generator.2015 Am Control Conf 2015:4735–40. <https://doi.org/10.1109/ACC.2015.7172075>.
- [13] Jia B. Analysis and control of a spark ignition free-piston engine generator. Newcastle University, 2016.
- [14] Boldea I. Linear Electric Machines, Drives, and MAGLEVs Handbook - Chapter 1. Linear Electric Machine. Drives, MAGLEVs Handb., Taylor & FrancisGroup;2013,p.1–34. <https://doi.org/10.1201/b13756-1>.
- [15] Mathworks. Simscape TM Language Guide. Mathworks 2020.
- [16] MathWorks. Using Simulink and Stateflow in Automotive Applications. MathWorks; n.d.
- [17] Krause PC, Wasynczuk O, Sudhoff SD. Analysis of Electrical Machinery and Drive Systems. A John Wiley & Sons; 2002.
- [18] Brosnan P, Tian G, Zhang H, Wu Z, Jin Y. Non-Linear and Multi-Domain Modelling of a Permanent Magnet Linear Synchronous Machine for Free Piston Engine Generators. Energy Conversion and Management X 2022;14:100195. <https://doi.org/10.1016/j.ecmx.2022.100195>.
- [19] Heywood JB. Internal combustion engine Fundamentals.NewYork,NY:McGrawHill;1988. [https://doi.org/10.1016/s1350-4789\(10\)70041-6](https://doi.org/10.1016/s1350-4789(10)70041-6).
- [20] Blair GP, Lau HB, Cartwright A, Raghunathan BD, Mackey DO. Coefficients of discharge at the aperaturesofengines.SAETechPaper 1995;104:2048–62.= <https://doi.org/10.4271/952138>.
- [21] Blair GP. Design and Simulation of Two-Stroke Engines. Warrendale: SAE; 1996.
- [22] Hohenberg GF. Advanced approaches for heat transfercalculations.SAETechPaper 1979;88:2788–806. <https://doi.org/10.4271/790825>.
- [23] Jia B, Zuo Z, Tian G, Feng H, Roskilly AP. Development and validation of a free-piston engine generator numerical model. Energy Conversion and Management 2015;91:333–41.<https://doi.org/10.1016/j.enconman.2014.11.054>.
- [24] Cockerill S. intelliGEN : Linear Generator platform technology 2021. <https://www.libertine.co.uk/>.